

---

# SPECT Imaging of Para-Axial Neurofibromatosis with Technetium-99m DTPA

Gerald A. Mandell, H. Theodore Harcke, Colleen Sharkey, Kevin M. Brooks,  
and G. Dean MacEwen

*Departments of Medical Imaging and Orthopedics, Alfred I. duPont Institute,  
Wilmington, Delaware*

Single photon emission computed tomography (SPECT) was used to study uptake of technetium-99m diethylenetriaminepentaacetic acid ( $^{99m}\text{Tc}$ ]DTPA) by para-axial neurofibromas in 13 patients. SPECT imaging led to better resolution of uptake in nine instances and detection of 12 lesions unsuspected on planar imaging (PI). Two false-positive instances and one false-negative instance of uptake are described. The planning of the surgical approach and placement of graft material for spinal fusion was assisted by SPECT in two patients. One patient with disability secondary to recurring abdominal pain had detection of the causative lesion by SPECT and subsequent relief of her symptoms following excision of the tumor. SPECT imaging of soft-tissue tumors of neurofibromatosis appears to have potential use in preplanning surgery on structural or cosmetic lesions, in the detection of occult lesions, and the monitoring of patients with neurofibromatosis at regular intervals.

J Nucl Med 28:1688-1694, 1987

---

The utilization of technetium-99m diethylenetriaminepentaacetic acid ( $^{99m}\text{Tc}$ ]DTPA) recently has been described as a means of locating occult neurofibromas throughout the body (1). The differentiation of isolated osseous dysplasia versus its coexistence with plexiform neurofibromas is a well-known diagnostic and clinical dilemma in patients with neurofibromatosis. Sometimes, flat neurofibromatous tissue in the paraspinal, mediastinal regions and even intra-abdominal locations is difficult to define or even suspect on plain radiography. Knowledge of the presence of this additional tissue can be helpful in preoperative planning of spinal fusions to avoid excessive bleeding. Because of the ability to image in a plane, we felt that SPECT had the potential to detect and resolve smaller, more subtle extrarenal soft-tissue collections of increased radioactivity than PI alone. Therefore, SPECT was added as an adjunct to PI in those patients with questionable plain radiographic findings or subtle planar scintigraphic results. This report deals with the effectiveness of SPECT for the detection of occult tumors in patients with neurofibromatosis.

## MATERIALS AND METHODS

The study population consisted of 13 patients with clinical stigmata of neurofibromatosis consisting of multiple cafe-au-lait spots, abnormal family history, proven biopsy, or characteristic osseous lesion (kyphoscoliosis or pseudoarthrosis of the tibia). There were seven males and six females, with ages ranging from 2.7 to 27.4 yr (mean 13.9 yr) (Table 1). The patients were scanned following an intravenous injection of  $^{99m}\text{Tc}$ ]DTPA at a dosage of 200  $\mu\text{Ci}/\text{kg}$  with a maximum dose of 10 mCi. The kidneys were evaluated in accordance with the established renal scintiscan procedure using a gamma camera equipped with a low-energy, all purpose collimator (LEAP). The routine study was modified according to the previously described neurofibromatosis scan protocol with different count statistics for various anatomic regions (thorax, abdomen 500,000 counts; head, neck, both extremities 300,000 counts; single extremity 150,000 counts) (1). Imaging of extrarenal portions of the body was begun 30 min after injection of the radiopharmaceutical and continued up to 3 hr postinjection. The 13 patients were selected for SPECT imaging to better define the extent of a clinically apparent soft-tissue process, confirm an area suspicious for disease on plain radiography or PI, or establish the cause of symptoms. SPECT scintigraphy was usually initiated in the second hour of the study because of the observation on PI of better tumor-to-background ratios during the second to fourth hours post-

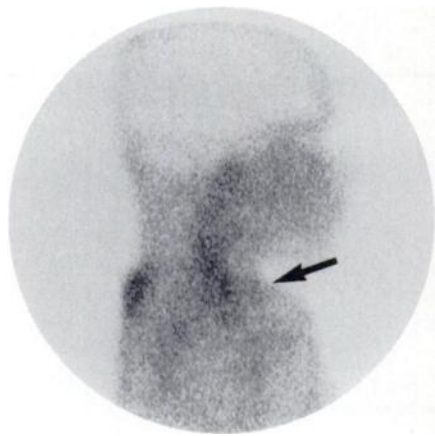
---

Received Aug. 19, 1986; revision accepted May 7, 1987.

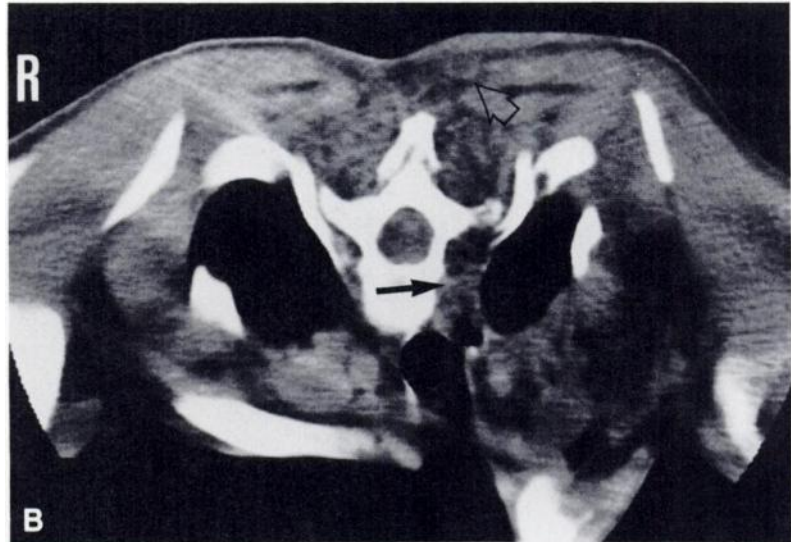
For reprints contact: Gerald A. Mandell, MD, Alfred I. duPont Institute, P.O. Box 269, Wilmington, DE 19899.

**TABLE 1**  
**Patient Summary**

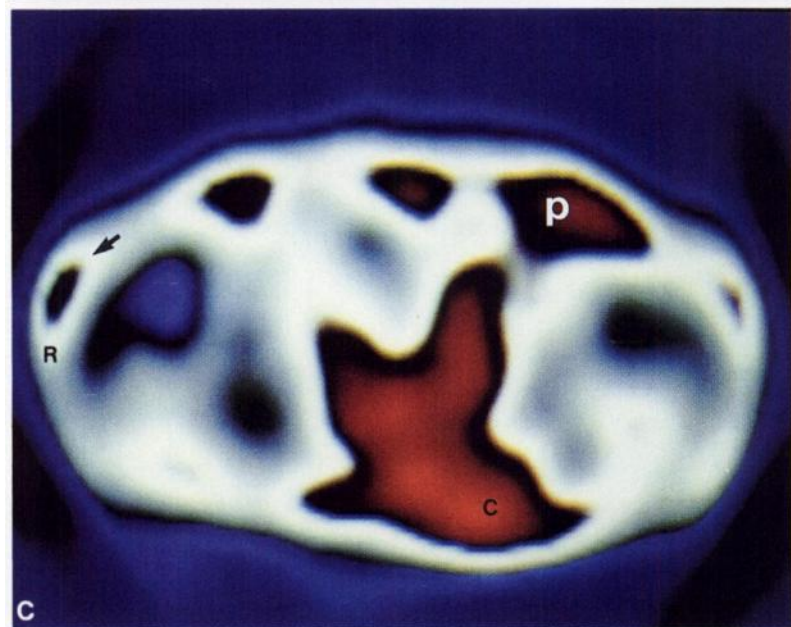
Patient no.	Age	Sex	Clinical information	X-ray findings	Planar findings	SPECT	Correlative imaging CT or MRI	Operation or biopsy
1	27 yr 5 mo	F	Scoliosis; Pre-op for spinal infusion	Kyphoscoliosis	? Left Cervical ? Left paraspinal Lower thoracic	+	+ (MRI) + (CT)	N/A N/A
2	3 yr 3 mo	F	Left exophthalmos	Sphenoid bone defect	Superficial left orbital region No activity sphenoid bone	+ -	+ (CT, MRI) -	N/A N/A
3	15 yr	F	Kyphoscoliosis; Pre-op for spinal infusion	Kyphosis Concave surfaces dorsal vertebrae	—	Anterior to thoracic kyphos	+ (CT)	+ (2.3 × 0.5 × 0.5 cm)
					—	Inferior to kyphos in upper lumbar	+ (CT)	N/A
4	11 yr 10 mo	M	Scoliosis	Scoliosis ? of soft tissue shadow	—	Mid-thoracic area	+ (CT)	N/A
5	14 yr 11 mo	M	Scoliosis	Scoliosis with associated scalloping	Right suprarenal	+	+ (CT)	N/A
					—	Paraspinal mid to lower thoracic	+ (CT)	N/A
					—	Anterior mediastinal	+ (CT)	N/A
6	7 yr	M	Enlarged left clavicle	Distorted uplifted left clavicle	Left anterior cervicothoracic Left posterior cervical	+ +	+ (CT) + (CT)	N/A N/A
7	26 yr 7 mo	M	Scoliosis	Scoliosis	—	Thoracic kyphos	+ (CT)	N/A
8	2 yr 9 mo	F	Facial asymmetry	Thickened left paraspinal soft tissue	—	Right lower anterior rib Right maxilla and mandible	+ (CT) + (CT)	N/A N/A
9	20 yr	M	Kyphoscoliosis; Pre-op fusion	Kyphoscoliosis	Right paravertebral lumbar area extend to left flank No activity anterior to lumbar spine	+ -	+ (CT) - (CT)	Subcutaneous plexiform thickened skin No significant tumor
						Upper lumbar ? intraspinal	+ (CT)	N/A
10	7 yr	M	Facial asymmetry asthma	Enlarged soft tissues of right face and neck	Right anterior cervical Right anterior face ? Anterior mediastinum ? Middle mediastinum ? Liver	+ + + +	+ (CT) + (CT) + (CT) + (U/S CT)	N/A N/A N/A N/A
11	14 yr 9 mo	M	Kyphoscoliosis	Kyphoscoliosis with large associated soft tissue mass	Anterior mediastinum Middle mediastinum Paraspinal	+ + +	+ (BE) + (CT) + (CT)	N/A N/A N/A
12	4 yr	M	Pseudoarthrosis	No paraxial abnormality	— — —	Left orbital Right cervical	- (CT) - (CT) + (CT) left cervical	N/A N/A
13	26 yr	F	Right abdominal and back pain	Sacral foraminal enlargement	Presacral	+	+ (CT)	N/A
					—	Right lower abdomen	+ (CT)	3.0 × 3.0 cm
					—	Superficial low back	+ (CT)	Subcutaneous lesions



**A**



**B**



**C**

**FIGURE 1**

**A:** Lateral planar scintigraph with slight activity anteriorly (arrow) and more intense uptake posteriorly. **B:** Transaxial SPECT image with soft tissue tumor (red) on left side extending from posterior (P) to anterior behind clavicle (C). Top of right shoulder (arrow) is visualized. **C:** Transaxial prone CT image with distorted left clavicle and adjacent disorganized soft-tissue planes, paraspinal capping of the left lung (arrow), and distortion of the subcutaneous fat plane posteriorly (open arrow), all secondary to plexiform neurofibroma infiltration.

injection of the radiopharmaceutical. Examinations were performed with a rotating gamma camera<sup>®</sup> equipped with a low-energy, all purpose collimator. Positioning was varied to include cephalo-cervical, thoracic or abdominal regions, according to areas suspicious for occult disease. The extent of tomography was also dependent on the size of the patient. All data was acquired and processed on 64 × 64 word matrices by the MDS A<sup>2</sup> computer. Sixty-four projections over 360° were acquired for 30 sec per projection. Following uniformity correction and filtering of the raw data (temporal and spatial both 11 pt,  $co = 0.2$ ), 6.2 mm thick transaxial, coronal, and sagittal tomograms were reconstructed. The sets of reconstructed images were evaluated independently and by simultaneous multiformated display. Contrast adjustments were made according to the degree of activity of the suspected lesion and interpretation was assisted by a color translation table (red = most active, gray = intermediate, blue = most inactive). In some instances, in order to visualize a small focus, an exaggeration of physiologic activity (bladder, ureters,

kidneys) occurred (Fig. 3C). The SPECT images were correlated predominantly with matching computed transaxial tomographic images (CT) of the affected areas (30 instances). In other instances, magnetic resonance imaging (MRI) (2), ultrasound (1), and plain radiography (1) were compared with the SPECT images.

Three additional patients with no evidence of neurofibromatosis who underwent renal scintiscanning for other reasons (pyelonephritis, neurogenic bladder, vesicoureteral reflux) served as controls for the delayed SPECT imaging. The control population consisted of two females and one male ranging in age from 15 to 21 yr (mean of 17 yr). SPECT acquisitions were obtained over a similar geographic area as the neurofibromatosis population with the same transaxial, sagittal, and coronal reconstructions. The images were used to establish the normal distribution patterns of [<sup>99m</sup>Tc]DTPA on the tomographic views and served as the standard when the neurofibromatosis patients were evaluated for abnormal paraxial extrarenal collections of activity.

## RESULTS

Single photon emission computed tomographic imaging of the control population established the normal pattern and contour of the physiologic distribution of [<sup>99m</sup>Tc]DTPA from the orbital regions to the lower abdomen. A relative increase in activity was seen in blood-pool locations (great vessels, heart, liver, spleen), redundant tissue (shoulder joints), and glandular tissues (thyroid, breasts, nasopharynx). Obviously, the most active areas were the kidneys and bladder. The presence of less activity in the stomach bubble and the osseous components of the spine resulted in areas of relative photopenia.

Areas of abnormally increased uptake on SPECT images were grouped according to location as orbital/facial, cervicothoracic, thoracic (anterior mediastinal, middle mediastinal, paraspinal, thoracic cage), and lumbosacral (paraspinal, intra-abdominal). Several areas of increased activity spanned more than one of the above specified locations and in this series received multiple compartmental listings. Ability to resolve areas of abnormally increased radiopharmaceutical uptake in different paraxial locations was determined (i.e., in the

**TABLE 2**  
Comparison of SPECT and PI in Detection of Soft-Tissue Tumors of Neurofibromatosis

	SPECT	PI
True-positive	28	16
True-negative	2	4
False-positive	2	0
False-negative	1	13
Sensitivity	97%	55%
Specificity	50%	100%
Accuracy	91%	61%

middle mediastinum physiologic cardiac blood-pool activity has to be separated from tumor activity) (Fig. 1). SPECT was compared with PI for locations of abnormal activity. The 13 patients were found to have 30 extra-renal sites of abnormal activity (orbital facial 4, cervicothoracic 5, thoracic 12, and lumbosacral 9) on the SPECT imaging of paraxial locations. Twenty-eight abnormal collections were confirmed by demonstration of abnormal soft tissue by other imaging modalities (CT, MRI, ultrasound, or plain radiography) and/or surgical excision or biopsy. As shown in Table 2, SPECT (0.97)

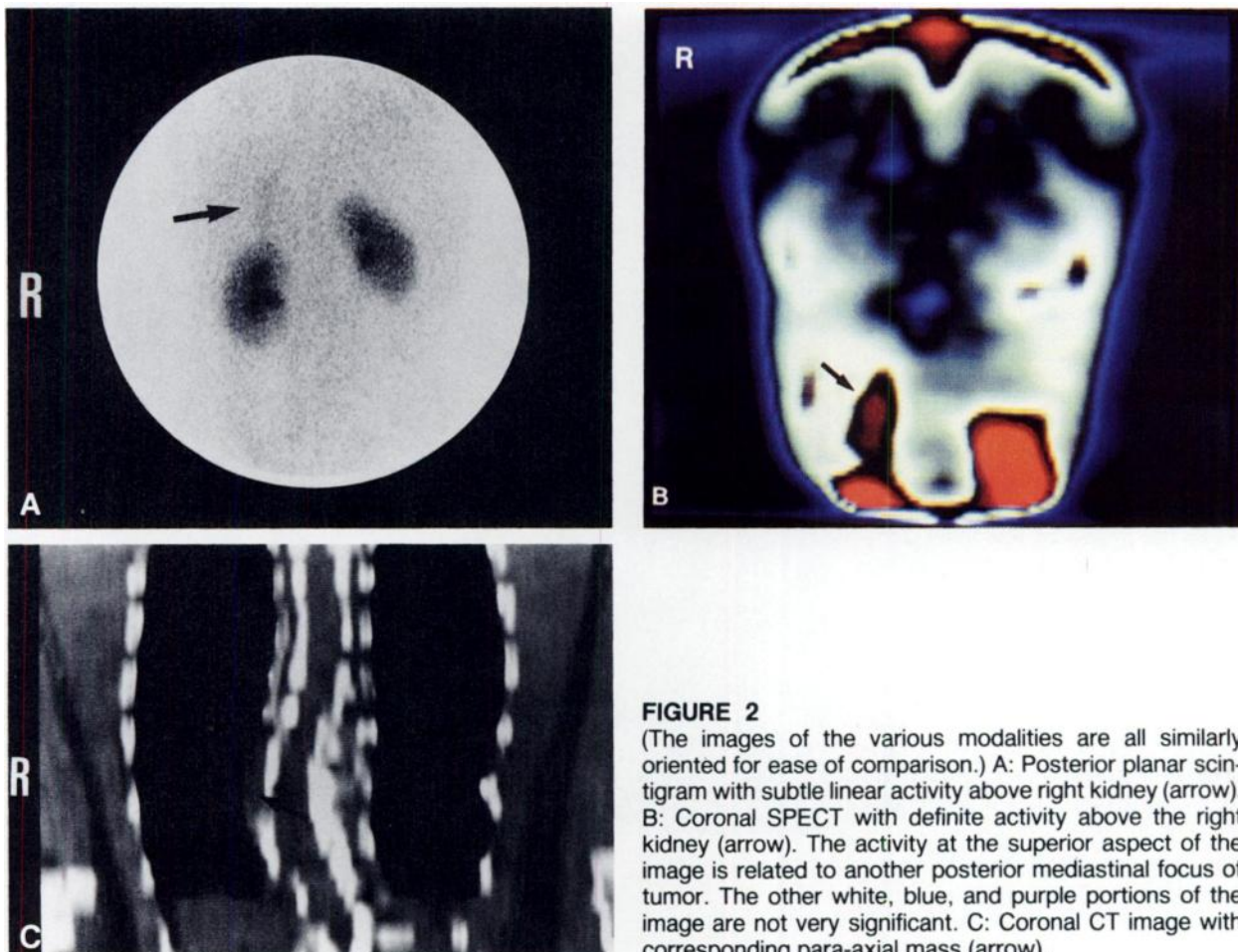


**FIGURE 2**  
(The images of the various modalities are all similarly oriented for ease of comparison.) A: Posterior planar scintigram with subtle linear activity above right kidney (arrow). B: Coronal SPECT with definite activity above the right kidney (arrow). The activity at the superior aspect of the image is related to another posterior mediastinal focus of tumor. The other white, blue, and purple portions of the image are not very significant. C: Coronal CT image with corresponding para-axial mass (arrow).

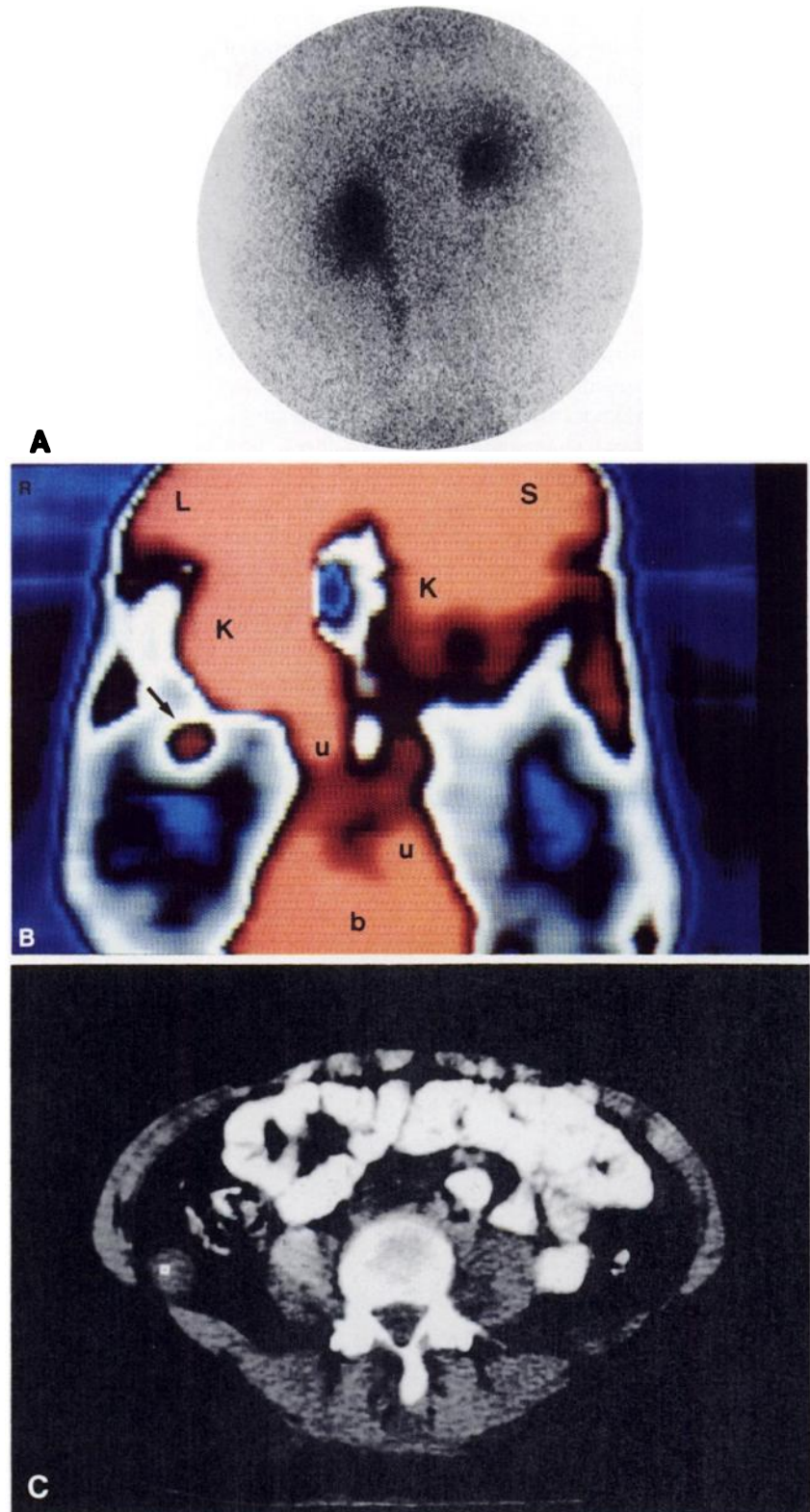


**FIGURE 3**  
 A: Planar image of abdomen demonstrating physiologic activity in kidneys but no focus of abnormal uptake. B: Coronal SPECT image with small round focus (arrow) on right side of abdomen. Kidneys (K), ureters (U), bladder (B), liver (L), and spleen (S) are overenhanced in order to display the small lesion. C: Transaxial CT image with neurofibroma (3.0 × 3.0 cm) located posteriorly (box) on the right side.

was more sensitive than PI (0.55). The specificity for SPECT and PI was 0.50 and 1.00, respectively.

SPECT was more accurate (0.91) than PI (0.61). SPECT imaging in nine instances led to increased resolution of lesions (Fig. 2) and the identification of 12 additional lesions unsuspected on planar imaging. Seven areas of dysplasia (spine 5, sacrum 1, clavicle 1) were confirmed as having associated soft-tissue tumors (Fig. 3). In one 4-yr-old patient, two false-positive sites and one false-negative site were observed. The right cervical area displayed increased uptake on SPECT. Computed tomographic examination revealed a prominent right thyroid lobe and a small neurofibroma (less than 8 mm and clinically unapparent) on the contralateral side. In the same patient, the left orbit exhibited increased activity. CT examination did not reveal a definite abnormality. Two patients with dysplasia (sphenoid bone defect and scalloped vertebrae in a kyphos) who had normal SPECT studies were confirmed by MRI or CT as being free of associated tumor.

Three patients in the study had surgery following their SPECT evaluation. In one patient, the planning of the surgical approach for anterior spinal fusion was significantly assisted by information gained preoperatively from the neurofibromatosis scan. As predicted by the scan, the area selected for thoracotomy was devoid of neurofibromas, the rib grafts were free of associated tumor, and the area of the anterior spinal fusion was easily accessible because no tumor resection was required. In a second patient undergoing spinal fusion the scan showed the presence of some neurofibromatous tissue at the inner margin of the dorsal kyphos. This small amount of tissue was confirmed at surgery. The third patient complained of persistent right sided abdominal and back pain. A round region of increased activity in the right lower abdomen was detected by SPECT and corroborated by CT. Removal of this neurofibroma resulted in relief of the patient's symptoms.

## DISCUSSION

Technetium-99m DTPA has been discovered to accumulate in the benign soft-tissue tumors of neurofibromatosis. Increased radiotracer uptake occurred in diffuse plexiform lesions as well as in well-circumscribed focal lesions (the smallest lesion detected on PI was a 1.5-cm subcutaneous nodule) (1).

Possible mechanisms of uptake of [<sup>99m</sup>Tc]DTPA in neurofibromas include necrosis active tumor uptake, protein binding, and blood-pooling secondary to increased capillary permeability and/or lack of normal venous drainage. Necrosis is unlikely as the mechanism. Bone-seeking isotopes usually localize in areas of necrosis. For instance, in myocardial necrosis, the combination of isotope delivery (residual blood flow) and salt deposition (calcium/phosphorous and/or hydroxyapa-

tite) allowing imaging of necrosis. Only one instance of bone radiotracer uptake in a neurofibroma has been reported in the literature (2). Our own experience with bone scintiscanning in four patients showed lack of uptake in neurofibromas of varying size. Neurofibromas are not usually hypervascular. The gradual rise in activity of several lesions was plotted on computer-generated time-activity curves (over a period of 30 min) (1). From our experience with PI of many lesions of varying sizes, there is gradual increase in activity and persistence of that activity for at least 4 hr postinjection of the radiopharmaceutical. There is, however, a small subgroup of hemangioneurofibromas that are extremely hypervascular and probably contribute to tissue overgrowth (elephantiasis). Because of our experience with one patient who had elephantiasis, we currently favor blood-pooling and not tumor cell uptake or protein binding as the explanation for uptake by neurofibromas. A preoperative scan demonstrated diffuse, patchy uptake in the patient's enlarged distal lower extremity. A biopsy of an area suspected to be malignant was performed, and the biopsy specimen was determined by well-counter to be four times as active as normal tissue. During the operation, a compression wrap was used to control excessive bleeding. When the patient was rescanned 1.5 hr following surgery, the abnormal collections of radioactivity had disappeared and the normal extremity had more background activity than the involved extremity. Presumably, the radioactivity was displaced out of the blood-pool regions by the compression procedure.

Technetium-99m DTPA uptake is not specific for neurofibromas; there are reports of localization in breast tumors (3), sarcomas (4), and a uterine myoma (5). In breast lesions, the intensity of uptake was the main differentiating feature between benign and malignant lesions (5). The possibility of differentiating malignant from benign tumors of neurofibromatosis has yet to be explored.

SPECT imaging has been found to improve the accuracy of scintigraphic detection of liver metastases ([<sup>99m</sup>Tc]sulfur colloid) (6), ischemic myocardium (thallium (7), mediastinal lymphoma (gallium) (8), and spondylolysis (bone scintigraphy) (9). SPECT imaging in our laboratory has allowed the detection of neurofibromas as small as 0.8 cm. The ability to detect lesions depends on their size and proximity to the camera (superficial versus deep). Small foci of abnormal extrarenal activity near areas of physiologic hyperactivity (kidneys, bladder, joints, breasts, thyroid, etc.) can be difficult to identify and may lead to false-negative results. The sensitivity (97%) of SPECT was certainly superior to the sensitivity (55%) of PI. A SPECT specificity of 50% is disappointing, but one must recognize that this is essentially a statistical phenomenon. Our small number of true-negative cases (2) does not reflect

the wide areas surveyed by the scan with no evidence of neurofibromatosis clinically or radiographically. We have no way of realistically expressing this as a discrete number of true-negative sites. With two false-positive cases, this adversely affects the calculation. The SPECT enhancement of the asymmetry of a physiologic structure, a prominent right thyroid lobe, resulted in one false positive. The thyroid activity is probably secondary to the gland's perfusion rather than free pertechnetate because the thyroid gland was not visible on PI. In the same patient, the left orbit enhancement was not explained by the negative CT examination. Perhaps the SPECT is predictive of ongoing microscopic metaplasia in the region. A repeat CT and/or MRI are scheduled for the upcoming year. The number of false-negative locations is also tenuous because scintigraphy encompasses a large body area and correlation with CT sections of the whole body segment would entail excessive irradiation. MRI correlation at this point is prohibitively expensive and time consuming. Overall, the accuracy of SPECT (91%) was quite promising when compared with PI (61%).

SPECT imaging of subtle para-axial neurofibromatosis with [<sup>99m</sup>Tc]DTPA appears encouraging for assisting orthopedic and plastic surgeons in preoperative planning, defining the presence of symptomatic occult neurofibromas, and sequentially following tumor growth in patients with neurofibromatosis.

#### NOTE

\* (General Electric 400AT) General Electric, Milwaukee, WI.

#### ACKNOWLEDGMENT

The authors thank Karen Moore for preparing the manuscript and Rod Hampton for producing the photographs.

#### REFERENCES

1. Mandell GA, Herrick WC, Hareke HT, et al. Neurofibromatosis: location by scanning with Tc-99m DTPA [Work in progress] *Radiology* 1985; 157:803-806.
2. Nolan NG. Intense uptake of 99m Tc diphosphonate by an extraosseous neurofibroma. *J Nucl Med* 1974; 15:1207-1209.
3. Cuschieri A, Hutchinson F, Neill GD, et al. Scintiscanning of the breast with 99Tcm- diethylene triamine penta-acetic acid, a prospective blind evaluation. *Br J Surg* 1981; 68:147-149.
4. Tyler JL, Powers TA. Tc-99m DTPA uptake in soft tissue sarcoma. *Clin Nucl Med* 1982; 7:357-358.
5. Lunia S, Lunia C, Philip PK, et al. Accumulation of Tc-99m-DTPA in uterine myoma. *Clin Nucl Med* 1980; 5:272-273.
6. Strauss L, Bostel F, Clorius JH, et al. Single-photon emission computed tomography (SPECT) for assessment of hepatic lesions. *J Nucl Med* 1982; 23:1059-1065.
7. Keyes JW Jr., Brady TJ, Leonard PF, et al. Calculation of viable and infarcted myocardial mass from thallium-201 tomograms. *J Nucl Med* 1981; 22:339-343.
8. Tumeh SS, Rosenthal D, Kaplan WD, et al. Comparison of Ga-67 planar imaging and single photon emission computed tomography in malignant chest disease [Abstract]. *J Nucl Med* 1985; 26:P111.
9. Collier EB, Johnson RP, Carrera GP, et al. Painful spondylolysis or spondylolisthesis studied by radiograph and single photon emission computed tomography. *Radiology* 1985; 154:207-211.